J. of Fire Prot. Engr., 6 (2), 1994, pp 79-87

MEASUREMENTS OF WATER DENSITY AND DROP SIZE DISTRIBUTIONS OF SELECTED ESFR SPRINKLERS

Tak-Sang Chan
Factory Mutual Research Corporation
Research Division
1151 Boston-Providence Turnpike
Norwood, Massachusetts USA 02062

SUMMARY

Characteristics of single sprinkler sprays for two Early Suppression Fast Response (ESFR) sprinklers were investigated. The water density, drop size and velocity distributions were measured at an elevation 2.85 m (9 ft 4 in.) below the sprinkler deflector for two water discharge pressures, 1.72 bar (25 psig) and 3.45 bar (50 psig). Measurements began at 0.61 m (2 ft) from the sprinkler axis and extended to near spray boundary. For every 0.61 m (2 ft) increment, the measurements were performed for 10 azimuthal angles with 45 degree intervals. The drop size and velocity distributions were measured with a PMS (Particle Measuring Systems, Inc.) optical imaging probe which can measure drop size ranging from 0.1 to 6.2 mm with a resolution of 0.1 mm.

The results of the water density measurements indicate that the water densities for the two sprinkler models diminish with increasing radial distance from the sprinkler axis. Based on the local measured density data, the gross density distributions in term of volume fraction for the entire sprinkler sprays were derived. It was found that the gross density distributions were well represented by the Rosin-Rammler equation. The distribution curves for the two sprinkler models discharging at 3.45 bar (50 psig) were close to each other.

From the drop size measurements, it was found that larger drops tended to be projected to near the spray boundary rather than towards the sprinkler axis. The average droplet velocity for each drop size was found to be very close to the experimental terminal velocity for a single water droplet traveling through air. The gross drop size distribution curves for the two sprinkler models were similar, with one model drop size distribution being uniformly smaller than the other. Each gross drop size distribution can be expressed as a combination of the log-normal equation and the Rosin-Rammler equation.

INTRODUCTION

The fire suppression effectiveness of a sprinkler depends on its capability to deliver a sufficient amount of water to a burning fuel surface to cool the surface and extinguish the fire. During a fire, the sprinkler spray must penetrate a hot fire plume, which is a gas-dynamic barrier above the burning fuel. For a given fire condition and fixed sprinkler arrangement, the water density and drop size distributions of a sprinkler spray are essential in controlling penetration of the spray to the fire seat. The spray must have sufficient water density and large droplets to prevent too much of the water drops being deflected by or evaporated in the up-flowing hot gas plume. An ideal sprinkler should render optimal distribution patterns which are tailored to the intended fire conditions.

In 1984, Factory Mutual Research Corporation (FMRC) initiated the Early Suppression Fast Response (ESFR) Research Program, resulting in the development of ESFR sprinkler models[1]. With ESFR sprinkler protection, high-challenge fires, such as a double-row rack storage fire of plastics up to 25 ft high, could be suppressed without the use of in-rack sprinklers. The objective of the present investigation was to quantify the spray characteristics in terms of water density and drop size distributions for two selected ESFR sprinkler models.

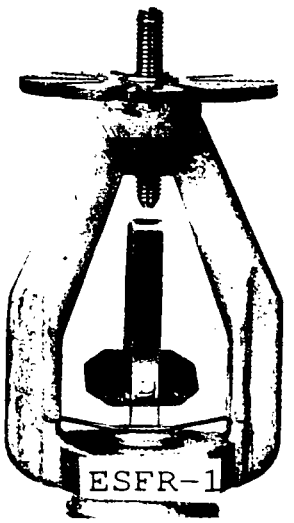

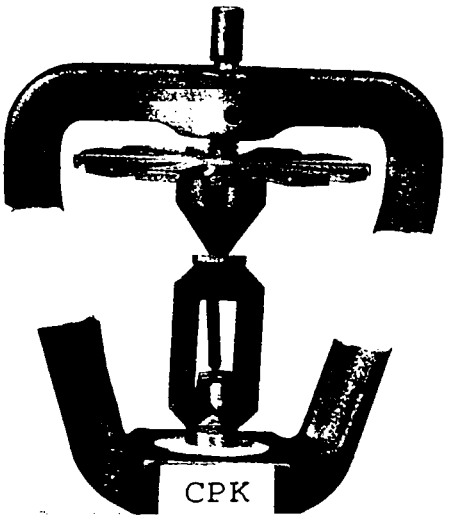

Figure 1: ESFR Sprinklers

MEASUREMENTS

The sprinkler water density and drop size distributions were measured at the FMRC Norwood test facility under a 9.93 m x 11.23 m suspended ceiling which was 4.6 m above the floor. The measurements were performed for two sprinkler models designated as CPK and ESFR-1; both have a nominal orifice diameter of 19 mm. Figure 1 shows a photograph of these sprinklers. For the CPK sprinkler model, measurements were performed for water pressures of 1.72 bar and 3.45 bar. For the ESFR-1 model, measurements were performed at 3.45 bar.

Figure 2: Drop Size Measurement Setup

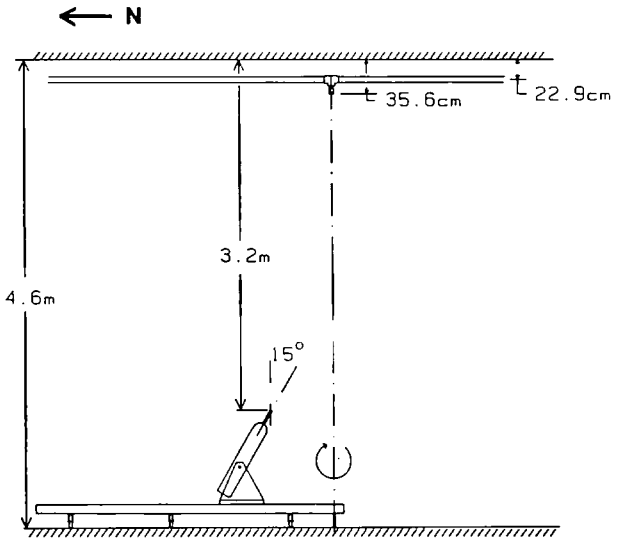

A single sprinkler pipe of 5.1 cm nominal diameter was installed horizontally 22.9 cm below the suspended ceiling, as shown in Figure 2, whereas the sprinkler deflector was leveled 35.6 cm below the ceiling. The two deflector-supporting arms of each sprinkler were aligned with the sprinkler pipe. The water flow in the sprinkler pipe could be turned on or off rapidly by a pneumatic valve situated at the inlet of each pipe. A pressure tap was installed at the downstream end of the sprinkler pipe to monitor the water stagnation pressures. The total water flow to the open sprinklers was also measured using a paddlewheel flow meter.

The drop size distributions were mapped out at a level of 3.2 m below the ceiling. The drop size probe was mounted on a platform, as shown in Figure 2, which could be traversed radially and azimuthally across the spray. The probe was fixed at an angle 15° from the vertical direction. A number of locations under the sprinkler were selected to perform the measurements. The measurement locations started at 0.61 m from the sprinkler centerline and extended to near the spray boundary. The farthest radial locations were 3.66 m from sprinklers when discharging at 1.72 bar

and 3.05 m at 3.45 bar, respectively. For every 0.61 m increment, the measurements were performed for 10 azimuthal angles with 45 intervals, except near the sprinkler pipe, where the interval was 25°. Figure 3 illustrates the measurement locations for water pressure of 1.72 bar.

Figure 3: Locations for Water Density and Drop Size Distribution Measurements: O Locations for both drop size and water density distribution measurements; ● Locations for water density measurements only.

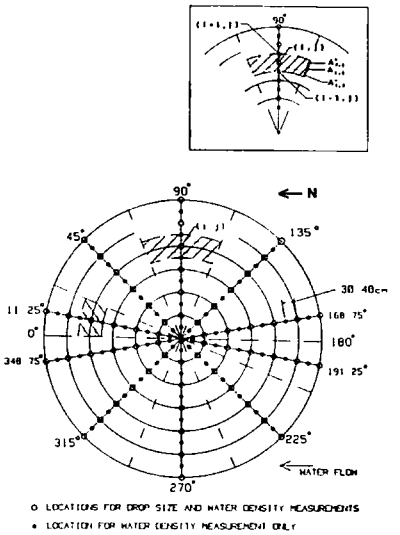

The drop size distributions were measured with the FMRC PMS Drop Size Measuring System (a high-speed drop sizing and counting system). This system is an optical imaging device. A He-Ne laser is used to project a beam of light as drops pass through the object plane of the optical system. The shadows behind the drops are projected onto a linear array of photodiodes to determine a slice of drop image by the number of shadowed photodiodes. As the drops pass through the laser beam, successive image slices are recorded. Two-dimensional drop images are then reconstructed with the recorded image slices. The drop size corresponds to the width of the widest image slice. The droplet velocity can be calculated based on the drop size and the droplet traveling time through the object plane of the probe. The imaging system can measure drop sizes ranging from 0.1 to 6.2 mm with a resolution of 0.1 mm. Additional information for the system can be found elsewhere[2].

The water density distributions were also measured at 3.2 m below the ceiling. Thirteen 30.48 cm x 30.48 cm x 30.48 cm deep pans were used to collect water. These pans were placed contiguously on the platform along the radial direction. Figure 3 also shows the locations for the water density distribution measurements.

Results and Data Analysis

In the following data analysis, the measurement area was divided into a number of zones such that each zone is centered to a measurement location, as shown by the hatched area in Figure 3. For the analysis of the drop size data, each zone is centered to a drop size measurement location and the area of the zone is bounded by the long dash lines as shown in the insert of Figure 3. For the water density data, each zone is centered to a density measurement location and the area is bounded by the dotted lines, also shown in the insert. The center of each zone is denoted with two indices, i and j. Index i denotes the i-th measurement position (or zone) in the radial direction from the sprinkler centerline, whereas j denotes the j-th azimuthal angle from the vertical plane of the deflector-supporting arm. The areas within each zone, also indicated in the figure, are denoted by $A_{i,j}^{+}$, $A_{i,j}$ and $A_{i,j}^{-}$.

Water Density Distributions

Figures 4, 5 and 6 show the azimuthal water density variation as a function of radial distance from the sprinkler axis. The abscissas are the azimuthal angles measured from the north side of the vertical plane of the sprinkler-deflector supporting arms (see Figure 3). To avoid overcrowding the data, only those results for the locations where both drop size and density measurements were made are presented in the figures. The water density variations are generally symmetrical to the plane of the deflector-supporting arms. Both sprinkler models appear to have such a distribution pattern that the water densities are maximum near the sprinkler and decrease with the radial distance from the sprinkler axis.

Figure 4: Azimuthal Water Density variation for Sprinkler Model CPK discharging at 1.72 bar (25 psi): Radial Distances from Sprinkler Axis —■— 0.61 m (2 ft); —▲— 1.22 m (4 ft); —◆— 1.83 m (6 ft); —▼— 2.44 m (8 ft); —●— 3.05 m (10 ft); —*— 3.66 m (12 ft).

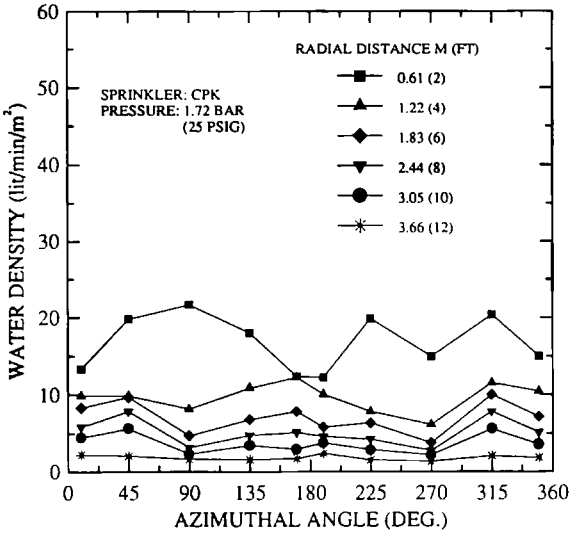

Figure 5: Azimuthal Water Density variation for Sprinkler Model CPK discharging at 3.45 bar (50 psi): Radial Distances from Sprinkler Axis —■— 0.61 m (2 ft); —▲— 1.22 m (4 ft); —◆— 1.83 m (6 ft); —▼— 2.44 m (8 ft); —●— 3.05 m (10 ft);

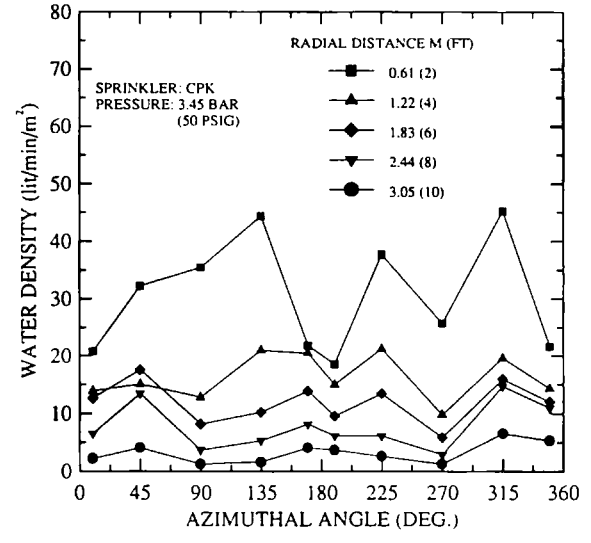

Based on the measured water density data, the gross cumulative distributions of the water density for the entire sprays can be derived. With the measurement area divided as described above, the gross cumulative distributions in term of volume fraction can be calculated as follows

Figure 6: Azimuthal Water Density variation for Sprinkler Model CPK discharging at 3.45 bar (50 psi): Radial Distances from Sprinkler Axis —■— 0.61 m (2 ft); —▲— 1.22 m (4 ft); —◆— 1.83 m (6 ft); —▼— 2.44 m (8 ft); —●— 3.05 m (10 ft);

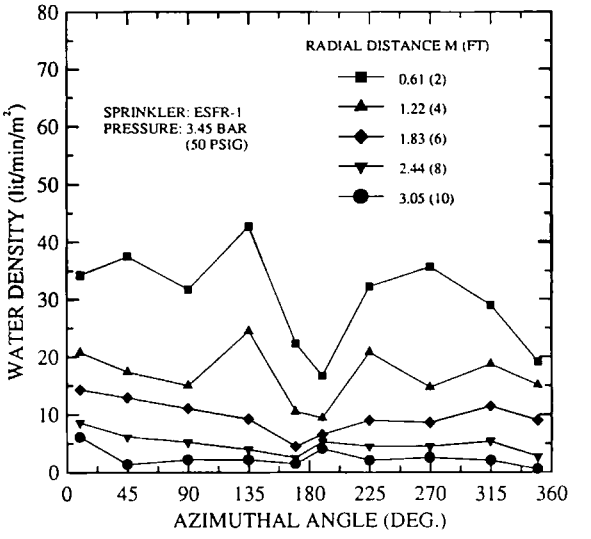

$$CVF_q = \frac{\sum_{q_{i,j} \le q} q_{i,j} A_{i,j}}{\sum_{i}^{N_I^*} \sum_{j}^{N_J^*} q_{i,j} A_{i,j}} \qquad (1)$$

where CVF_q is the cumulative volume fraction of water collected with densities below or equal to a water density of q; $q_{i,j}$ is the measured water density at position (i, j) and $A_{i,j}$ the corresponding zone area as shown in Figure 3. N_I^* and N_J^* are the number of density measurement locations in the radial and azimuthal directions, respectively. It was assumed that the measured density at position (i, j) represented the average density over the entire area of each zone.

With an interval of 2 lit/min/m² for q in Equation 1, the cumulative density distributions derived using Equation 1 are shown in Figure 7. As seen in the figure, the cumulative distributions for the two sprinkler models compare closely with each other. The cumulative distributions were fitted with the Rosin-Rammler equation and the results are also presented in Figure 7. The Rosin-Rammler equation can be expressed as

$$CVF_q = 1 - e^{-0.693\left(\frac{q}{q_m}\right)^{\gamma}} \quad (2)$$

where q_m corresponds to the median water density. The values of q_m and γ in Equation 2 were determined by least-square fitting of Equation 2 to the reduced data. It is seen that the CVF_q for the present data are well represented by the Rosin-Rammler equation. Table 1 presents the values of q_m and γ, which provide the best fits of data.

Table 1

GROSS VOLUMETRIC MEDIAN DIAMETER (q_m) AND THE VALUES OF γ FOR THE DENSITY DISTRIBUTION

Sprinkler Model	Discharge Pressure (bar)	q_m (lit/min/m²)	γ
CPK	1.72	5.87	1.56
CPK	3.45	13.2	1.89
ESFR-1	3.45	12.7	1.34

Figure 7: Gross Water Density Distribution Fitted with Rosin-Rammler Distribution: ● Model CPK at 1.72 bar (25 psi); O Model CPK at 3.45 bar (50 psi); □ Model ESFR-1 at 3.34 bar (50 psi); ——— Rosin-Rammler Distribution.

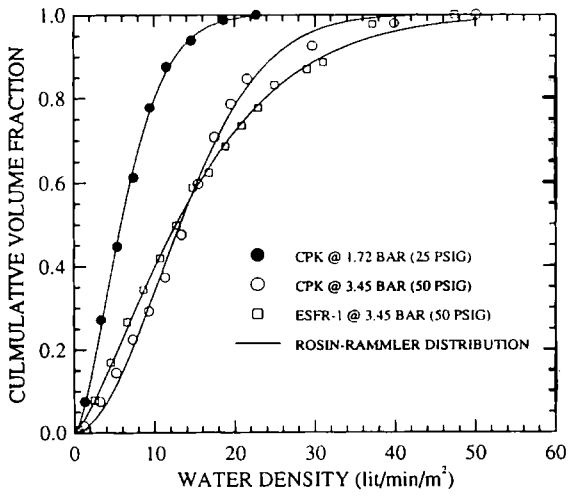

Drop Size Distributions

The results of the drop size measurements are presented in Figures 8, 9 and 10, which contain the spatial variations of the local volumetric median diameters for the two investigated sprinkler models. In general, the local volumetric median diameters increase with the radial distance and vary slightly with the azimuthal angles.

After dividing the measurement area as described in the beginning of this section, the overall water flow rate for each zone, $W_{i,j}$, may then be approximated as:

$$W_{i,j} = A^{-}_{i,j}\, q_{i-1,j} + A_{i,j}\, q_{i,j} + A^{+}_{i,j}\, q_{i+1,j} \quad (3)$$

where the areas $A_{i,j}$, $A_{i,j}^{-}$ and $A_{i,j}^{+}$ are indicated in Figure 3. The drop size distribution between the (i-1)-th and (i+1)-th radial positions, $CVF_{i,d}$, is then

$$CVF_{i,d} = \frac{\sum_{j}^{N_J} W_{i,j}\, CVF_{i,j,d}}{\sum_{j}^{N_J} W_{i,j}} \quad (4)$$

Figure 8: Local Volumetric Median Diameter variation for Sprinkler Model CPK discharging at 1.72 bar (25 psi): Radial Distances from Sprinkler Axis ——■—— 0.61 m (2 ft); ——▲—— 1.22 m (4 ft); ——◆—— 1.83 m (6 ft); ——▼—— 2.44 m (8 ft); ——●—— 3.05 m (10 ft); ——✳—— 3.66 m (12 ft).

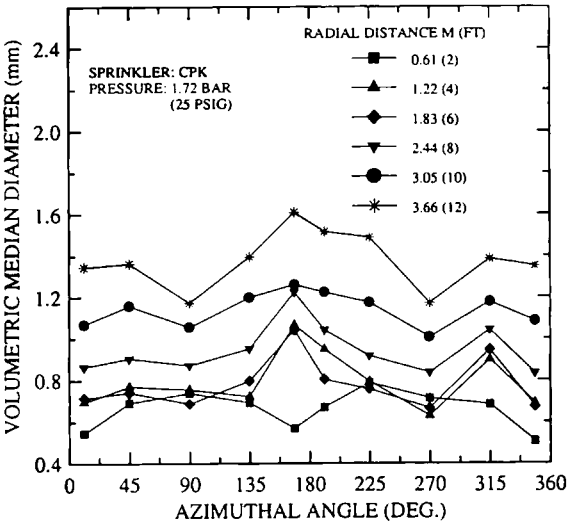

and the gross drop size distribution, CVF_d, for the entire measurement area is

$$CVF_d = \frac{\sum_{i}^{N_I} \sum_{j}^{N_J} W_{i,j} \, CVF_{i,j,d}}{\sum_{i}^{N_I} \sum_{j}^{N_J} W_{i,j}} \qquad (5)$$

where $CVF_{i,j,d}$ is the local cumulative volume fraction for water below or equal to a drop size, d, at the i-th radial and j-th azimuthal position. N_I and N_J are the numbers of drop size measurement locations in the radial and azimuthal directions, respectively. As before, it was assumed that the measured data at position (i, j) represented the average value over the entire area of each zone.

Figures 11 to 13 show the results of the calculation for $CVF_{i,d}$. Both sprinkler models tend to project larger drops to the outer area than near the sprinkler axis, regardless of water discharge pressures. Figure 14 presents the gross drop size distributions calculated using Equation 5 for the two sprinkler models. As expected, the figure shows that the higher the discharge pressure, the smaller the droplets generated by the sprinkler. Also seen in the figure, the two models have similar gross drop size distributions. However, droplets produced by the ESFR-1 sprinkler model are uniformly smaller than those of the CPK model.

Figure 9: Local Volumetric Median Diameter variation for Sprinkler Model CPK discharging at 3.45 bar (50 psi): Radial Distances from Sprinkler Axis
—■— 0.61 m (2 ft);
—▲— 1.22 m (4 ft); —◆— 1.83 m (6 ft);
—▼— 2.44 m (8 ft); —●— 3.05 m (10 ft);

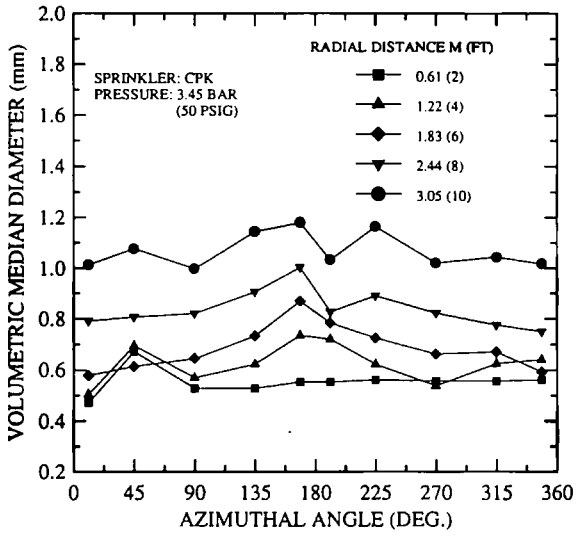

Figure 10: Local Volumetric Median Diameter variation for Sprinkler Model ESFR-1 discharging at 3.45 bar (50 psi): Radial Distances from Sprinkler Axis
—■— 0.61 m (2 ft);
—▲— 1.22 m (4 ft); —◆— 1.83 m (6 ft);
—▼— 2.44 m (8 ft); —●— 3.05 m (10 ft);

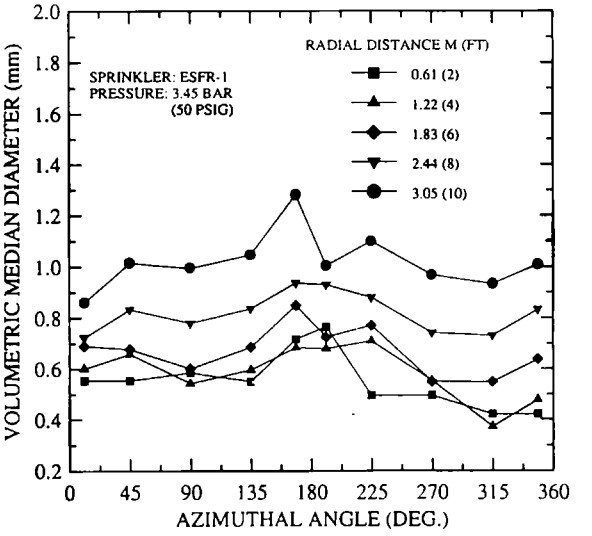

Figure 11: Drop Size Distribution for Sprinkler Model CPK discharging at 1.72 bar (25 psi): Radial Distances from Sprinkler Axis —■— 0.61 m (2 ft);
—▲— 1.22 m (4 ft); —◆— 1.83 m (6 ft);
—▼— 2.44 m (8 ft); —●— 3.05 m (10 ft);
—*— 3.66 m (12 ft).

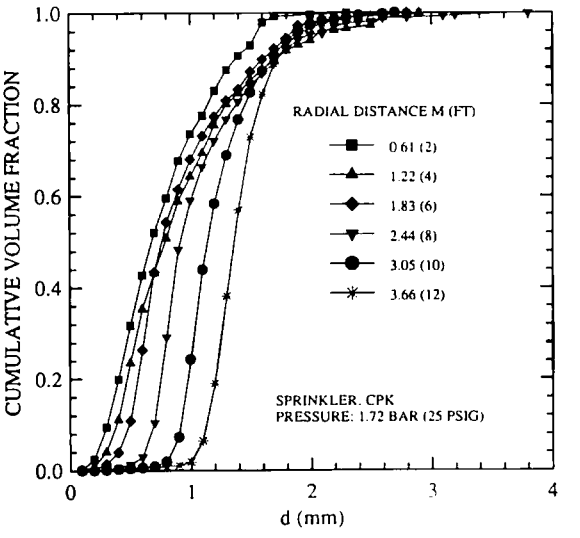

It has been found previously that the gross drop size distributions for sprinkler sprays can be expressed with two different distribution equations in two respective drop-size ranges[3]; one is the log-normal equation for $d < d_m$; the other is the Rosin-Rammler equation for $d \geq d_m$. The expressions of cumulative volume fraction based on the log-normal equations is:

$$CVF_d = \frac{1}{(2\pi)^{\frac{1}{2}}} \int_0^d \frac{1}{\sigma x} e^{-\frac{[\ln(\frac{x}{d_m})]^2}{2\sigma^2}} d(x) \qquad (6)$$

for $d < d_m$, and for $d \geq d_m$ CVF_d can be expressed by Equation 2 with q and q_m replaced by d and d_m, respectively. Least-square regression analysis was performed on the reduced data, and the results are also shown in Figure 14. The values of σ and γ for the best fits of data are listed in Table 2.

Figure 13: Drop Size Distribution for Sprinkler Model ESFR-1 discharging at 3.45 bar (50 psi): Radial Distances from Sprinkler Axis —■— 0.61 m (2 ft); —▲— 1.22 m (4 ft); —◆— 1.83 m (6 ft); —▼— 2.44 m (8 ft); —●— 3.05 m (10 ft);

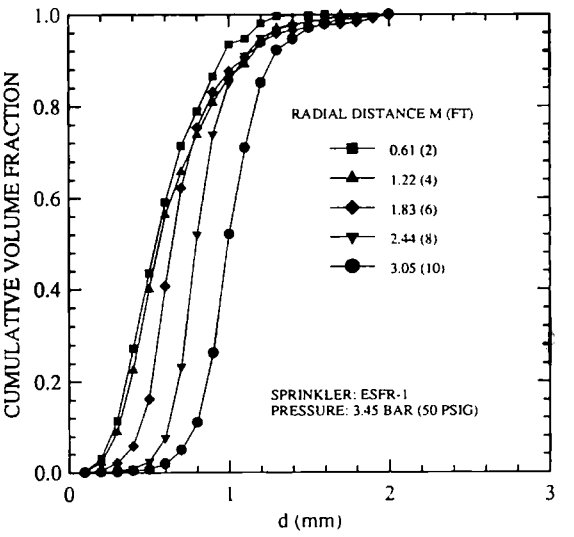

Figure 12: Drop Size Distribution for Sprinkler Model CPK discharging at 3.45 bar (50 psi): Radial Distances from Sprinkler Axis —■— 0.61 m (2 ft); —▲— 1.22 m (4 ft); —◆— 1.83 m (6 ft); —▼— 2.44 m (8 ft); —●— 3.05 m (10 ft);

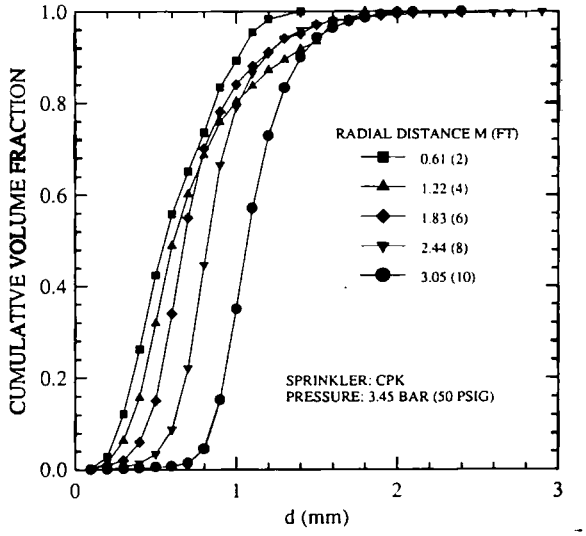

Figure 14: Gross Drop Size Distribution Fitted with Rosin-Rammler and Log-Normal Distributions: □ Model ESFR-1 at 3.45 bar (50 psi); ○ Model CPK at 3.45 bar (50 psi); ● Model CPK at 1.72 bar (25 psi); ------ Rosin-Rammler Distribution; ——— Log-Normal Distribution.

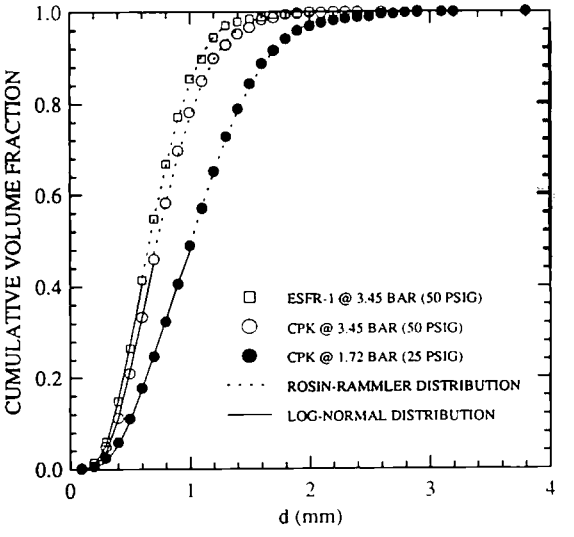

Table 2

GROSS VOLUMETRIC MEDIAN DIAMETER (d_m) AND THE VALUES OF σ AND γ FOR THE DROP SIZE DISTRIBUTION

Sprinkler Model	Discharge Pressure (bar)	d_m (mm)	σ	γ
CPK	1.72	1.01	0.58	2.43
CPK	3.45	0.72	0.51	2.34
ESFR-1	3.45	0.67	0.50	2.43

Water Droplet Velocity

The water droplet velocity component in the direction of the probe cylinder (see Figure 2) was derived based on the traveling distance, which is equal to the measured drop size for spherical drop, and the measured traveling time through the object plane of the optical probe. Figure 15 shows the velocity component averaged for each drop size class. For comparison, the experimental terminal velocity[4] for a single water droplet traveling through air is also included in the figure. As seen in the figure, the water droplets of the two ESFR sprinkler sprays were traveling at the terminal velocity under the present measurement conditions.

Figure 15: Water Droplet Velocities in Comparison with Experimental Terminal Velocities: O Model CPK at 3.45 bar (50 psi); □ Model CPK at 1.72 bar (25 psi); Δ Model ESFR-1 at 3.45 bar (50 psi); —●— Experimental Terminal Velocity (Ref.4).

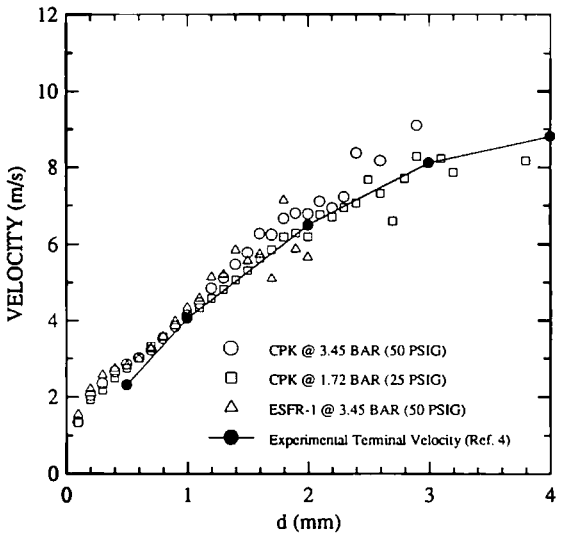

Summary and Conclusion

Water density distributions and drop size distributions have been measured for two ESFR sprinklers at 2.85 m below the sprinkler deflector. The measurement locations covered an area which started at a distance 0.61 m from the sprinkler axis and ended near the spray boundaries. Measurements were performed at discharge pressures of 1.72 bar and 3.45 bar. Several observations and findings from the present investigation are summarized as follows:

(1) The water density distributions for the two ESFR sprinklers were found to be roughly symmetrical to the plane containing the two deflector-supporting arms, and to decrease with increasing radial distance from the sprinkler axis.

(2) The gross water density distributions in term of volume fraction for the two sprinkler models are close to each other. Each distribution curve is well correlated with the Rosin-Rammler equation.

(3) The local volumetric median diameter increases with the radial distance, decreases with the sprinkler discharge pressure and varies slightly with the azimuthal angles.

(4) The gross drop size distribution curves for the two ESFR sprinkler models are similar, with one model drop size being uniform smaller than the other.

(5) Each gross drop size distribution can be expressed with the log-normal distribution for drop size smaller than the volumetric median diameter and with the Rosin-Rammler distribution for drop size greater than the volumetric median diameter

(6) For the present arrangement tested, the measured droplet velocity compares closely to the terminal velocity for a single water droplet traveling through air.

Acknowledgments

The author would like to thank Dr. H-C Kung for encouragement and discussion during the course of this work. The valuable suggestions provided by Dr. H-Z Yu are gratefully acknowledged. Special thanks are extended to Mr. W. R. Brown for designing and constructing the probe-traversing system and for assistance in conducting the experiments. The author also thanks Mr. E. E. Hill for assistance in constructing the probe-traversing system.

NOMENCLATURE

$A_{i,j}$	area as defined in Figure 3
$A_{i,j}^-$	area as defined in Figure 3
$A_{i,j}^+$	area as defined in Figure 3
$CVF_{i,j,d}$	local cumulative volume fraction for water below or equal to a drop size, d, at position (i, j)
$CVF_{i,d}$	cumulative volume fraction for water below or equal to a drop size, d, at a radial distance r_i
CVF_d	gross drop size distribution
CVF_q	gross water density distribution
d	drop diameter
d_m	volumetric median diameter
i	index to the measurement location in the radial direction
j	index to the measurement location in the azimuthal direction
N_I^*	number of water density measurement locations in the radial direction
N_J^*	number of water density measurement locations in the azimuthal direction
N_I	number of drop size measurement locations in the radial direction
N_J	number of drop size measurement locations in the azimuthal direction
q	water density
q_m	volumetric median water density
$q_{i,j}$	local measured water density at position (i, j)
$W_{i,j}$	overall water flow rate in zone centered to position (i, j)
x	dummy variable in Equation 6
σ	constant in Equation 6
γ	constant in Equation 2

REFERENCES

1. Yao, C., "The Development of the ESFR Sprinkler System," *Fire Safety Journal*, 14, pp. 65-73, 1988.
2. Yu, H-Z. and Symonds, A. P., "Sprinkler Drop-Size Measurements, Part I: An Investigation of the FMRC PMS Drop-Size Measuring System," FMRC Technical Report, J. I. 0G1E7.RA, 1982.
3. Yu, H-Z., "Investigation of Spray Patterns of Selected Sprinklers with the FMRC Drop Size Measuring System," *Proceedings of the 1st International Symposium on Fire Safety Science*, Hemisphere Publishing Corp., 1986, pp. 1165-1176.
4. Yao, C., "Effect of Drop Size on Sprinkler Performance," FMRC Technical Report, J. I. 18792, 1970.